Influence of Pr doping and oxygen deficiency on the scattering behavior of $YBa_2Cu_3O_7$ thin films

I. François
Interuniversitair Micro-Elektronica Centrum, Kapeldreef 75, B-3001 Leuven, Belgium

C. Jaekel and G. Kyas
Institut für Halbleitertechnik II, RWTH Aachen, Sommerfeldstr. 24, 52056 Aachen, Germany

D. Dierickx and O. Van der Biest
Departement Metaalkunde en Toegepaste Materiaalkunde, K.U. Leuven, 3001 Leuven, Belgium

R. M. Heeres
Interuniversitair Micro-Elektronica Centrum, Kapeldreef 75, B-3001 Leuven, Belgium

V. V. Moshchalkov and Y. Bruynseraede
Laboratorium voor Vaste-Stof-Fysika en Magnetisme, K.U. Leuven, Celestijnenlaan 200D, 3001 Leuven, Belgium

H. G. Roskos
Institut für Halbleitertechnik II, RWTH Aachen, Sommerfeldstr. 24, 52056 Aachen, Germany

G. Borghs
Interuniversitair Micro-Elektronica Centrum, Kapeldreef 75, B-3001 Leuven, Belgium

H. Kurz
Institut für Halbleitertechnik II, RWTH Aachen, Sommerfeldstr. 24, 52056 Aachen, Germany

(Received 6 July 1995; revised manuscript received 3 November 1995)

A comparative study of the complex conductivity and the scattering behavior of Pr-doped and oxygen deficient $YBa_2Cu_3O_7$ thin films with varying Pr or oxygen content is performed using terahertz coherent time-domain spectroscopy in combination with dc-resistivity measurements. Both Pr doping and removal of oxygen decrease the hole concentration in the CuO_2 planes. The specific conductivity behavior measured from 300 to 8 K shows two phase transitions: the superconducting transition at the critical temperature and a transition that can be explained by a suppression of the spin wave (spinon) density below the spin gap temperature. The nearly identical scattering behavior observed for both types of doping is discussed in the framework of P.W. Anderson's theory. [S0163-1829(96)06418-1]

I. INTRODUCTION

Doping is an important parameter to study the characteristics of the complex conductivity $\sigma(T)$ of high-T_c oxides. Substitution of Pr for the Y atom in YBaCuO, or Zn and Co for the Cu atoms in the CuO_2 planes and CuO chains, respectively, or removal of oxygen from the CuO chains influences the hole content (Pr, O, Co) or the hole mobility (Zn) in the planes.

Several models have been proposed to explain the scattering behavior in the high T_c oxides. In these models, the main scattering mechanism is based on spin fluctuations (antiparamagnon model[1]) or on a combination of spin and charge fluctuations (marginal Fermi liquid model).[2–4] These models can explain the unusual T-linear resistivity behavior in the normal state, believed to be a consequence of the linear temperature dependence of the quasiparticle scattering rate $1/\tau$. Moreover, calculations have shown that these spin fluctuations can give rise to high-temperature superconductivity.[5,6]

A phenomenological approach to describe the normal state properties is given by Anderson in his resonating valence bond (RVB) theory, [7–10] who separates spin and charge into two types of quasiparticle excitations: the holons (bosons) that carry charge and no spin and the spinons (fermions) that carry spin and no charge. Charged particles (holons) are almost solely scattered by spinons, which leads to a linear $\sigma(T)$ temperature behavior in the normal (strange metal) state. Spinons can also be scattered by spinons which is observed as a transverse scattering rate in Hall measurements. In the mean-field approximation of the RVB theory,[11] two characteristic temperatures related to two phase transitions govern the physics. On the one hand the spin gap temperature T_g below which the spin degrees of freedom (spinons) condense to form Zhang-Rice singlets, and on the other hand the Bose-Einstein condensation temperature T_{BE} below which the charge degrees of freedom (holons) become paired and Bose condense. A general mean-field phase diagram for the HTSC's as a function of hole doping has been proposed, [12] that will be used here because our data fit very well within this scheme as discussed later. The occurrence of

a gap in the spin excitations yields a deviation from the T-linear conductivity behavior as already observed in oxygen deficient[13,14] and Pr-doped samples.[15] The spin gap temperature T_g depends on the Pr or O content in the $Y_{1-x}Pr_xBa_2Cu_3O_y$ system. The spin gap formation in the cuprates has been further explored by Ubbens and Lee,[16,17] who attribute it to strongly enhanced pairing of spinons in adjacent CuO_2 planes. The in-plane pairing of the spinons is shown to be completely destroyed by a fluctuating gauge field, whereas the interplane pairing is much less sensitive to this gauge field and hence can give rise to the opening of the spin gap.

In various high frequency measurements on undoped $YBa_2Cu_3O_7$ a broad maximum in the real part of the conductivity as a function of temperature has been observed below T_c.[18,19] This maximum differs from the sharp peak near T_c observed at frequencies of about 10 GHz,[20,21] attributed to a distribution of slightly different T_c's in the sample. Within the two fluid model used here to extract the normal conductivity $\sigma_1(T)$, the occurrence of the broad peak is attributed to a competition between an increase in the normal carrier relaxation time and a decrease in the number of normal carriers with decreasing temperature below T_c.[1] The narrow peak disappears at THz frequency[20] improving the interpretation of our measurements.

High-frequency measurements offer a way to study systematically the conductivity in the whole temperature range, going (in the underdoped system) from above T_g to below the critical temperature T_c. In this work we study the influence of Pr doping and oxygen deficiency on the complex conductivity and scattering rate of YBCO thin films in the terahertz regime and compare these results with dc measurements.

II. EXPERIMENT

The $Y_{1-x}Pr_xBa_2Cu_3O_y$ layers are prepared by laser ablation on $NdGaO_3$ substrates from Pr-doped targets with $0 \leqslant x \leqslant 0.4$. $NdGaO_3$ is chosen as the substrate, because it is untwinned, in contrast with $LaAlO_3$, that has a highly twinned structure and influences the transmitted signals in a nonreproducible way. The Pr-doped samples have a T_c of 88, 78, 65, and 52 K, respectively, for $x=0$, 0.1, 0.2, and 0.3. For the preparation of oxygen deficient specimens, the oxygen content of the $YBa_2Cu_3O_y$ samples is reduced by performing an anneal and subsequent cooling in a controlled oxygen pressure, following a constant oxygen content line in the oxygen pressure vs temperature (pT) phase diagram.[22] Three samples are prepared to have an oxygen content y of about 6.80, 6.65, and 6.40, yielding a T_c of 75, 55, and 17 K. All samples are measured by x-ray diffraction to verify the c-axis orientation and to assure that they have a satisfactory crystal quality. As expected, the c-axis of the oxygen-depleted layers increases with increasing oxygen deficiency. The absolute oxygen content is determined from the pT diagram used for the preparation and confirmed through determination of T_c by four-probe dc-resistivity measurements.

The ultrahigh frequency measurements are performed by time-domain THz spectroscopy as described in Refs. 23,24. This technique permits the determination of the THz-frequency complex transmissivity even in the case of extremely thin superconductor films and without the need for patterning of the sample. Analysis of the Fourier spectra yields the absolute value of the real and imaginary part of the conductivity over a broad frequency range. Coherent THz-radiation pulses are generated by excitation of an InP surface emitter with 100-fs optical pulses derived from a self-modelocked Ti:sapphire laser. Time-resolved detection of the THz pulses transmitted through the sample is achieved with a 50-μm-long photoconductive dipole antenna that is gated by a time-delayed portion of the laser beam.[25] The frequency range useful for further Fourier evaluation ranges from 200 GHz to about 2 THz in the measurement reported here. To eliminate the influence of substrate absorption and dispersion, we measure both the transmissivity of the sample (superconductor plus substrate) and of the $NdGaO_3$ substrate alone. From the data, we determine the complex transmission coefficient

$$t(\omega)=\frac{E_t(\omega)}{E_t^0(\omega)}=\frac{1+n}{1+n+Z_0\sigma(\omega)}, \tag{1}$$

where n is the refractive index of the substrate and $E_t^0(\omega)$ is the transmitted electric field from the reference measurements with the substrate alone. With the known film thickness d, the absolute values of both the real and imaginary part of the conductivity $\sigma(T)$ are evaluated from $t(\omega)$.[26] Since all films are c-axis oriented, the measured conductivity refers to the carrier mobility in the ab plane only. The absolute $\lambda(T)$ values are obtained by fitting the imaginary part of the conductivity with the expression $\sigma_2(T)=1/\omega\mu_0\lambda(T)^2$.

III. RESULTS AND DISCUSSION

The dc-resistivity curves as a function of temperature for both the Pr-doped and the oxygen deficient samples are depicted in Fig. 1. All the resistivity curves show a deviation from the linear T dependence below the spin gap temperature T_g, where the slope of the resistivity becomes steeper with decreasing temperature. The temperature T_g where the deviation occurs, increases with increasing Pr doping or oxygen deficiency, consistent with earlier observations.[13–15] We also see a deviation from the linear behavior for the undoped sample at about 120 K, although for a sample with optimum hole doping the spin gap temperature should coincide with the critical temperature T_c following the mean-field phase diagram. This discrepancy is possibly due to the fact that the undoped film does not have a maximum T_c.

The real component of the THz conductivity σ_1 at 1 THz for the Pr-doped series of samples is shown in Figs. 2(a) and 2(b). All $\sigma_1(T)$ data of the different samples show the same behavior. First, from 300 K down to T_g a $1/(a+bT)$ behavior is present. At T_g, $\sigma_1(T)$ deviates from this temperature dependence with decreasing temperature reaching a maximum at a certain temperature below T_c. The $\sigma_1(T)$ peak has a lower amplitude for samples with a lower T_c, which is related to a higher Pr doping and consequently a lower hole content in the CuO_2 planes. The rise of the experimental conductivity data starting at the spin gap temperature is only slightly influenced by the superconducting transition at T_c. The scattering rate governing the conductivity seems to decrease monotonically, starting from the spin gap temperature, through the superconducting transition.

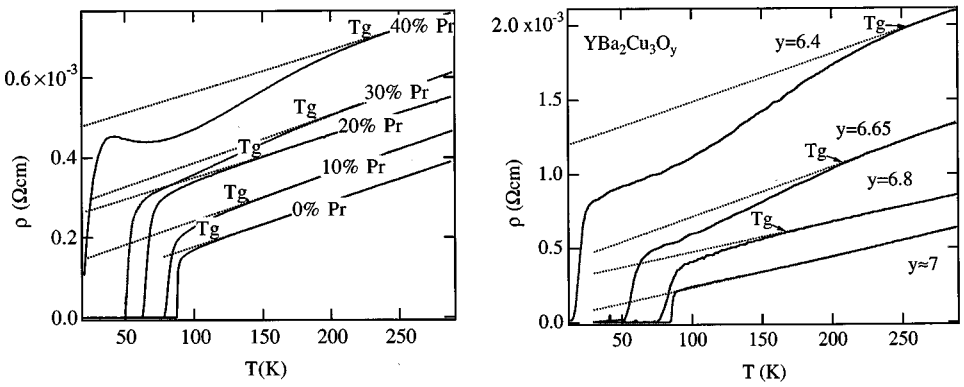

FIG. 1. dc resistivity of Pr-doped and oxygen deficient samples.

The temperature dependence of σ_1 is completely determined by the temperature dependence of the number of normal carriers and the scattering rate $1/\tau$. In order to estimate the general temperature dependence of the scattering rate, we fitted the σ_1 data with the expression

$$\sigma_1(T) = C \times \tau(T) \times x_n(T), \tag{2}$$

with C a temperature independent constant. The variation of the normal fluid fraction x_n ($x_n + x_s = 1$) with temperature below T_c is deduced from the temperature dependence of the penetration depth λ, which determines the fraction of paired carriers.

Above the spin gap temperature T_g, $1/\tau$ changes linearly with temperature in agreement with theory; the normal fluid fraction is 1 at temperatures down to T_c. Below T_c, the normal fluid fraction is given by

$$x_n(T) = \left[[1 - x_n(0)] \left(1 - \frac{\lambda(0)^2}{\lambda(T)^2} \right) \right] + x_n(0). \tag{3}$$

For the scattering rate $1/\tau$ at temperatures lower than T_g, we propose the expression

$$1/\tau(T) \sim \exp(T/T_0), \tag{4}$$

with T_0 and $x_n(0)$ introduced as fit parameters.

The decrease of the relaxation rate $1/\tau$ due to singlet pairing of the spinons is taken to be exponential, in analogy with the observed exponential temperature dependence of the nuclear spin/lattice relaxation rate in YBaCuO.[1] In a perfect superconductor, the real part of the conductivity for $T \to 0$ K is expected to approach zero because of the vanishing normal-carrier density. Since this is not the case here, we introduce $x_n(0)$ as a temperature independent contribution which accounts for the residual fraction of carriers that have not condensed at $T = 0$. This $x_n(0)$ fraction is present in every YBaCuO sample and is to some extent related to the quality of the sample. The relative magnitude of this fraction was verified for different Pr concentrations with a microwave cavity measurement of the (effective) surface resistance at 87 GHz, as shown on Fig. 3. The residual surface resistance measurement shows the same trend as the high frequency measurement with a larger residual uncondensed fraction at higher doping, i.e., at lower T_c. This residual fraction is sometimes subtracted from the conductivity data as a temperature independent part of the conductivity.[18] This gave an unsatisfying fit to our data. The residual fraction $x_n(0)$ scatters like the temperature-dependent normal carrier fraction (quasiparticles) and was consequently multiplied with the exponential function of the scattering time. This however leads to an artificial upturn at the lowest temperatures because in our fit procedure we assume $1/\tau$ only influenced by spin scattering, rather than by inelastic particle-phonon or particle-particle scattering. That assumption leads to an artificial infinite scattering length at 0 K and the observed upturn.

We also neglect the influence of the condensation of quasiparticles on relaxation times or spinon singlet formation below the critical temperature. This is in contrast to previous models,[1] in which was assumed that the decrease in $1/\tau$ below T_c follows from the decrease in quasiparticle density. If

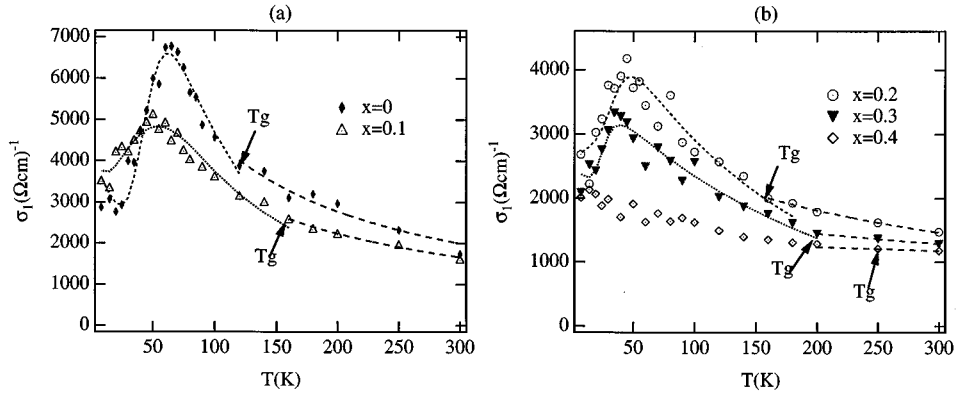

FIG. 2. (a,b) Real part of the conductivity at 1 THz as a function of the temperature for $Y_{1-x}Pr_xBa_2Cu_3O_7$. The dashed and dotted lines are the fitted curves following the simplified Drude formula.

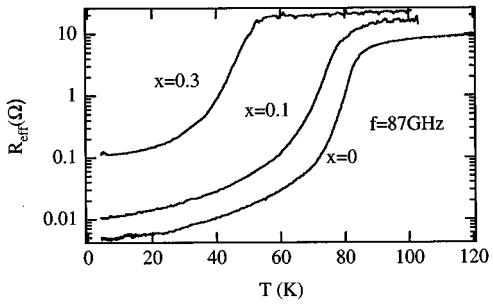

FIG. 3. Surface resistance measurement of $Y_{1-x}Pr_xBa_2Cu_3O_7$ at 87 GHz.

the influence exists it may be large for low Pr-doped samples with the largest amount of quasiparticles. If spinon pairing is influenced by the holon condensation any interpretation of the data below T_c based on the two fluid model is very complicated and our data do not allow such a refined analysis. However, in samples with a low T_c and a large T_g our approach is justified as reflected by the data, because the temperature separation between T_c and T_g is large. In between no holon condensation takes place. In Figs. 2(a) and 2(b) the fitting curves following the above discussed formulas are shown, with T_0 and $x_n(0)$ as fit parameters summarized in Table I together with the spin gap temperature T_g and the critical temperature T_c. If we compare the T_0 values with T_g, we see that they follow the same trend and have comparable values at different Pr concentrations.

This analysis of the THz-conductivity data shows that two independent mechanisms are responsible for the normal state resistivity and the superconducting transition, as was already suggested by Anderson.[27] The superconducting transition only influences the conductivity by decreasing the number of normal carriers, but it does not affect the way they are scattered. The position of the maximum in the conductivity is completely determined by the normal carrier content, which is dependent on T_c. That explains why all the conductivity peaks coincide when scaled with T_c.

The obtain a rough estimate of the absolute value of the scattering rate, the conductivity data can be fitted with a modified Drude formula, according to Bonn *et al.*[18]:

$$\sigma_1 = \frac{\tau}{\mu_0 \lambda(0)^2 (1+\omega^2\tau^2)} x_n \tag{5}$$

and

$$\sigma_2 = \frac{\tau^2 \omega}{\mu_0 \lambda(0)^2 (1+\omega^2\tau^2)} x_n + \frac{1}{\mu_0 \lambda(0)^2 \omega} x_s, \tag{6}$$

TABLE I. Critical temperatures deduced from the dc measurements and parameters from the fits in Fig. 2.

x	T_c	T_0	T_g	$x_n(0)$
0	88	82	115	0.25
0.1	78	127	145	0.48
0.2	65	151	155	048
0.3	52	188	190	0.7

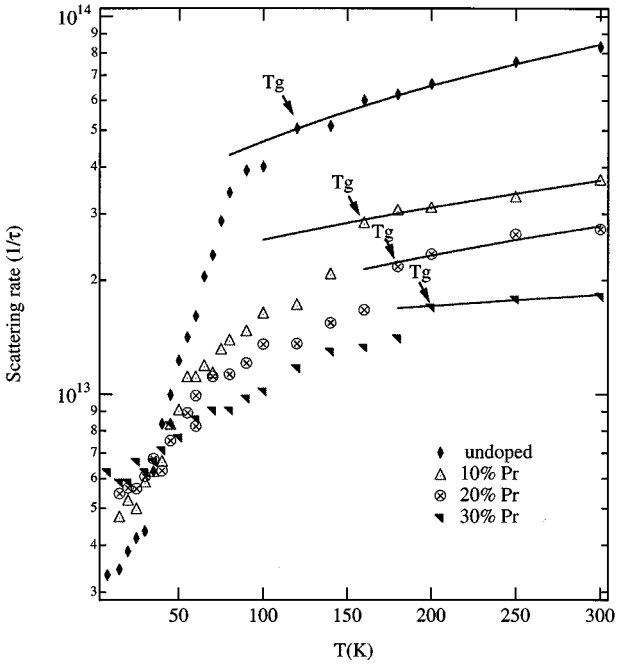

FIG. 4. Quasiparticle scattering rate $1/\tau$ at 1 THz for the Pr-doped samples.

where ω is the angular frequecy of the incident radiation; x_n and x_s are the temperature-dependent normal and superconducting fluid fraction, respectively.

The penetration depth $\lambda(0)$ in Eqs. (5) and (6), obtained from the σ_2 data, represents the total number of carriers (or the plasma frequency) in an indirect way. It is assumed for this approximation that all carriers are condensed at $T=0$. The effect of setting $x_n(0)=0$ leads to an overestimation of the penetration depth $\lambda(0)$ and an underestimation of the carrier number or plasma frequency.

In Fig. 4 the resulting scattering rate of the Pr-doped samples is displayed as a function of temperature in a semilogarithmic plot. A clear steplike drop is observed in the scattering rate at the spin gap temperature, below which the scattering rate starts to decrease faster with temperature. The slope of the curves below T_g becomes smaller for higher Pr concentrations, compatible with the increase of T_0 with increasing doping found in the fitting results of Table 1. The scattering rate above the spin gap temperature is linear with T and decreases continuously with increasing Pr doping. This decrease of the scattering rate with increasing Pr doping is surprising, if we consider the results from infrared-reflectivity measurements on oxygen deficient crystals.[28] They report an increasing scattering rate with reduced oxygen content, a result which is clearly inconsistent with our results for Pr-doped YBaCuO.

We have to be careful, however, when comparing the absolute level of the scattering rate for the different Pr concentrations, due the error in the determination of the carrier number, as indicated above. Moreover, it has been suggested that the two fluid model may not be completely adequate to deduce the scattering rate from the conductivity data.[29]

The oxygen deficient samples show the same conductivity behavior as Pr-doped samples as shown in Fig. 5. The real part of the conductivity of both series of doped samples can

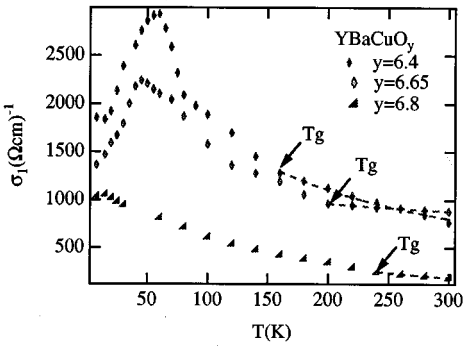

FIG. 5. Real part of the conductivity at 1 THz as a function of temperature for O-deficient samples.

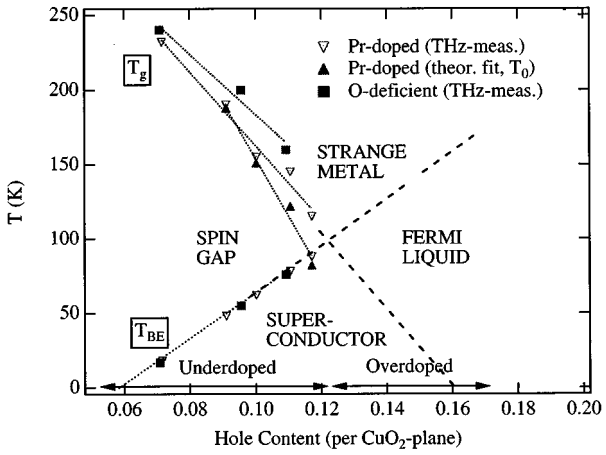

FIG. 7. Phase diagram showing T_g and T_{BE} (T_c in the underdoped region) of Pr-doped and O-deficient YBCO.

be scaled with T_c as shown in Fig. 6, and it is found that all curves reach their maximum at about 0.8 T_c. The coincidence of the scaled conductivity peaks below T_c in both the Pr-doped and the oxygen deficient samples and the similar exponential decrease of the scattering rate below the spin gap temperature indicates that the fundamental scattering mechanism does not change when we add praseodymium or remove oxygen.

In Fig. 7 we represent the data of the Pr-doped and the oxygen deficient samples in the mean-field phase diagram. The hole content for the different doped samples is calculated from the T_c values following an experimentally determined universal T_c-hole content relation for the high-T_c oxides, as was proposed in Ref. 30. We observe that as a function of temperature for a fixed Pr concentration or oxygen content two phase transitions take place in going from the strange metal phase to the superconducting phase via the spin gap phase.

To stress the relationship between T_g and T_0 we have added both values to the diagram. It is also clear from this figure that the spin gap temperatures found for a fixed T_c are similar in both components. In this analysis, the Bose-Einstein temperature T_{BE} is identified with the observed critical temperature T_c, since for underdoped samples superconductivity sets in at T_{BE}, following the phase diagram.

Alternatively the spin scattering mechanism and the spin gap phenomenon are described by a model developed by Sokol,[31] in which the existence of two types of low energy excitations in the high-T_c cuprates is proposed: antiferromagnetic (AF) spin waves (spinons) which carry spin-1 and no charge and Fermi-liquid-like quasiparticles which carry spin-1/2 and charge e. The scattering behavior is again determined by scattering of the quasiparticles by the spinons. In the completely insulating parent compounds of YBaCuO and LaSrCuO, where long range AF order exists, only spin waves are present; in the overdoped compounds the quasiparticles form the only excitations. In the strange metal phase, both excitations are present, but the contribution of the quasiparticles to the spectral weight of the low energy excitations is very small in comparison with the spin wave contribution. The spin gap is originating from a suppression of the low frequency spectral weight for the spin waves: at frequencies below the spin gap $\omega<\Delta=c/\xi$ (with c the spin wave velocity and ξ the magnetic correlation length), only the quasiparticle contribution is left, above the gap frequency both spin waves and quasiparticles contribute. Upon increasing hole doping (higher T_c), the spin gap increases because the magnetic correlation length ξ decreases. Although this phenomenological analysis looks very attractive, it implies a spin gap temperature which increases with increasing hole doping, in contrast with our experimental observations.

The observation that the conductivity behavior of Pr-doped $YBa_2Cu_3O_7$ is similar over the whole temperature range leads to the affirmation that the only influence of the Pr ion is depleting carriers from the CuO_2 planes. If magnetic pair breaking would be the origin of the suppression of T_c, as was proposed previously,[32] we should see a difference in

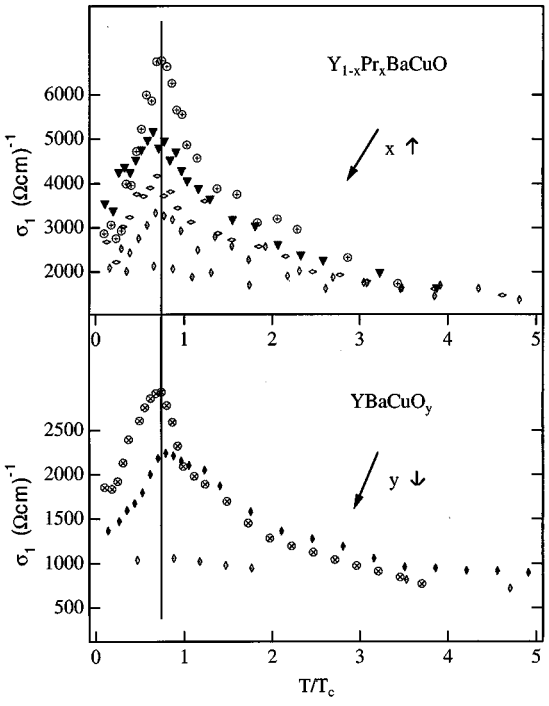

FIG. 6. Real part of the conductivity at 1 THz as a function of the temperature for Pr-doped (upper part) and O-deficient YBCO (lower part) scaled with T_c.

the conductivity behavior below the critical temperature. From these measurements, in which we are able to check the interplay between the superconductor and the magnetic impurity in the superconducting state, it seems that the magnetic properties of the Pr ion are not of importance here. About the mechanism of the carrier depletion by Pr, we cannot draw conclusions from these experiments; hole filling by a tetravalent Pr ion,[33] hole localization,[34–36] or transfer of the holes from the Cu-O $pd\sigma$ band into a new state [Fehrenbecher-Rice (FR) state] originating from Pr-O hybridization[37,38] all remain valid possibilities.

A second proof of the change in carrier concentration upon adding Pr is obtained by comparing the normal state Hall angle as a function of doping in both Pr-doped and O-deficient samples. In the framework of his spin-charge separation theory, Anderson has discussed the normal state Hall angle in the high-T_c oxides when in-plane impurities are introduced.[7,39] One can distinguish two different electronic relaxation times: the transport relaxation time discussed above and a transverse relaxation time which shows a quadratic temperature dependence ($\tau_H \propto T^{-2}$). The transport relaxation time is determined by scattering between holons and spinons, while the transverse relaxation time depends on scattering between spinons alone. The Hall angle is only dependent on τ_H, following $\cot(\Theta_M) \propto 1/\tau_H \propto T^2$. Since spinons can interact with magnetic impurities (bound spinons), the final formula for the transverse scattering rate is

$$1/\tau_H = T^2/W_s + 1/\tau_M , \tag{7}$$

where W_s is the bandwidth of the spin excitations, which is of the order of the superexchange constant J, and $1/\tau_M$ the temperature independent impurity contribution. The Hall angle cotangent is then

$$\cot\Theta_M = \alpha T^2 + C, \tag{8}$$

with C the temperature independent impurity contribution. The slope of the Hall angle cotangent shows the proportionality

$$\alpha B \propto \frac{n}{W_s}, \tag{9}$$

with n the carrier density. This theory has already been applied to Zn-doped and oxygen deficient YBaCuO films. Zn as a dopant does not significantly change the carrier concentration in the planes;[39] the Hall angle of $YBa_2Cu_{3-x}Zn_xO_7$ shows a T^2 dependence with a constant slope but with a systematic increase of the temperature independent contribution C with increasing Zn content, indicating the presence of local spin impurities due to the Zn doping.[40] For oxygen deficient $YBa_2Cu_3O_y$ films, a systematic decrease of the slope was observed with decreasing oxygen content.[14] The temperature independent contribution C remained nearly constant for $y \leqslant 6.6$ and increased suddenly for lower oxygen contents, accompanied by a sudden drop in the mobility. Wuyts *et al.* observed a linear relationship between the product αB and the hole content in the material, and concluded that applying Anderson's theory the superexchange J (or the spinon bandwidth) should remain constant as a function of hole doping.

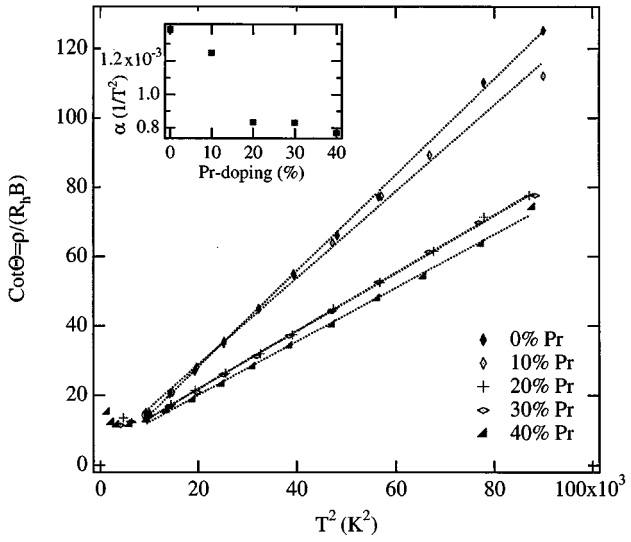

FIG. 8. Hall angle for Pr-doped films calculated with the Hall number data of Matsuda *et al.*

We estimated the Hall angle behavior for the Pr-doped layers using our resistivity data and the Hall-number data published by Matsuda *et al.*[41] In Fig. 8 the Hall angle cotangent is shown for the different Pr concentrations. The T^2 behavior is clearly present, as well as a slope variation as a function of doping. The slope decreases with increasing Pr doping, in a similar way as has been observed for the oxygen deficient samples. The intercept $C = \cot\Theta_H$ ($T = 0$ K) remains practically constant as a function of doping.

When we classify the different doped oxides following their Hall cotangent behavior, two main groups can be distinguished: the oxides in which the carrier density in the CuO_2 planes is unaffected, exhibiting a constant slope of the Hall cotangent as a function of temperature, and the oxides in which the carrier density is modified by doping, showing a Hall cotangent with a doping dependent slope. Both the Pr-doped and oxygen deficient $YBa_2Cu_3O_y$ samples, as well as, e.g., Co-doped $YBa_2Cu_{3-x}O_7$,[42] belong to the second group in this classification (Co substitutes for Cu^{2+} in the chains and depletes carriers in the planes), while Zn- and Ni-doped samples follow the first picture. These two groups of doped oxides can also be distinguished when we consider the magnetic properties: Pr-doped and oxygen deficient $YBa_2Cu_3O_7$ show a long range antiferromagnetic ordering at high Pr contents or high O deficiency, whereas this ordering does not occur in Zn-doped $YBa_2Cu_3O_7$.[43]

IV. CONCLUSIONS

Pr-doped and O-deficient $YBa_2Cu_3O_7$ exhibit a similar conductivity behavior as a function of doping, for temperatures below and above T_c. All samples exhibit a peak in the real part of the THz conductivity as a function of temperature, at a value of about $0.8^* T_c$. The peak in the conductivity can be understood in a model that predicts the suppression of the low energy spin excitations, and hence of the relaxation rate, below the spin gap temperature. Above the spin gap temperature, which is doping dependent, both the dc

resistivity and THz conductivity curves are linear in temperature. The superconducting transition has no significant influence on the scattering rate, which suggests that the normal state resistivity and the superconducting transition are governed by two different, independent mechanisms.

The spin gap temperature is similar for a fixed T_c in both types of doped samples, indicating that the spin gap is completely determined by the carrier density. The similarity between both types of samples indicates that the only effect of the Pr ions is the depletion of mobile carriers in the CuO_2 planes, whereas the magnetic character of the Pr ion does not have any influence on the superconductivity.

The similar T dependence of the Hall angle as a function of Pr doping or O deficiency, analyzed with Anderson's model, as opposed to, e.g., Zn-doped $YBa_2Cu_3O_7$, yields further evidence for this observation.

ACKNOWLEDGMENTS

We thank S. Hensen and H. Piel of the Bergische Universität Wuppertal for the microwave cavity measurement. This work was supported by the Belgian Impulse Programme for High Temperature Superconductivity and the German Bundesministerium für Forschung und Technologie under Contract No. 13N6288. I.F. is financially supported by the Flemish IWT.

[1] B.W. Statt and A. Griffin, Phys. Rev. B **46**, 3199 (1992).
[2] C.M. Varma, P.B. Littlewood, S. Schmitt-Rink, E. Abrahams, and A.E. Ruckenstein, Phys. Rev. Lett. **63**, 1996 (1989).
[3] P.B. Littlewood and C.M. Varma, J. Appl. Phys. **69**, 4979 (1991).
[4] E.J. Nicol and J. Carbotte, Phys. Rev. B **44**, 7741 (1991).
[5] P. Monthoux, A.V. Balatsky, and D. Pines, Phys. Rev. Lett. **67**, 3448 (1991).
[6] P. Monthoux and P. Pines, Phys. Rev. Lett. **69**, 961 (1992).
[7] P.W. Anderson, Phys. Rev. Lett. **67**, 2092 (1991).
[8] P.W. Anderson, G. Baskaran, Z. Zou, J. Watley, T. Hsu, B.S. Shastry, B. Douclot, and S. Liang, Physica C **153-155**, 527 (1988).
[9] P.W. Anderson and Z. Zou, Phys. Rev. Lett. **60**, 132 (1988).
[10] P.W. Anderson, Science **235**, 1196 (1987).
[11] G. Baskaran, Z. Zou, and P.W. Anderson, Solid State Commun. **63**, 973 (1987).
[12] N. Nagaosa and P.A. Lee, Phys. Rev. B **45**, 10 719 (1992).
[13] T. Ito, K. Takenaka, and S. Uchida, Phys. Rev. Lett. **70**, 3995 (1993).
[14] B. Wuyts, E. Osquigil, M. Maenhoudt, S. Libbrecht, Z.X. Gao, and Y. Bruynseraede, Physica C **222**, 341 (1994).
[15] R. Buhleier, S.D. Brorson, I.E. Trofimov, J.O. White, H.-U. Habermeier, and J. Kuhl, Phys. Rev. B **50**, 9672 (1994).
[16] M.U. Ubbens and P.A. Lee, Phys. Rev. B **49**, 6853 (1994).
[17] M.U. Ubbens and P.A. Lee, Phys. Rev. B **50**, 438 (1994).
[18] D.A. Bonn, R. Liang, T.M. Riseman, D.J. Baar, D.C. Morgan, K. Zuang, P. Dosanjh, T.L. Duty, A. MacFarlane, G.D. Morris, J.H. Brewer, W.N. Hardy, C. Kallin, and A.J. Berlinsky, Phys. Rev. B **47**, 11 314 (1993).
[19] M.C. Nuss, P.M. Mankiewich, M.L. O'Malley, E.H. Westerwick, and P.B. Littlewood, Phys. Rev. Lett. **66**, 3305 (1991).
[20] A.A. Golubov, M.R. Trunin, S.V. Shulga, D. Wehler, J. Dreibholz, G. Müller, and H. Piel, Physica C **213**, 139 (1993).
[21] T. Shibauchi, A. Maeda, H. Kitano, T. Honda, and K. Uchinokura, Physica C **203**, 315 (1992).
[22] E. Osquigil, M. Maenhoudt, B. Wuyts, and Y. Bruynseraede, Appl. Phys. Lett. **60**, 1627 (1992).
[23] M. Nuss, P.M. Mankievich, M.L. O'Malley, E.H. Westerwick, and P.B. Littlewood, Phys. Rev. Lett. **66**, 3305 (1991).
[24] C. Jaekel, C. Waschke, H. Roskos, H. Kurz, W. Prusseit, and H. Kinder, Appl. Phys. Lett. **64**, 3326 (1994).
[25] P. Smith, D. Auston, and M. Nuss, IEEE J. Quantum Electron. **QE-24**, 255 (1988).
[26] M. Nuss, K. Goossen, P. Mankiewich, and M. O'Malley, Appl. Phys. Lett. **58**, 2561 (1991).
[27] P.W. Anderson, Phys. Today **47**, 11 (1994).
[28] L.D. Rotter, Z. Schlesinger, R.T. Collins, F. Holtzberg, C. Field, U.W. Welp, G.W. Crabtree, J.Z. Liu, Y. Fang, K.G. Vandervoort, and S. Flesher, Phys. Rev. Lett. **67**, 2741 (1991).
[29] O. Klein, Phys. Rev. Lett. **72**, 1390 (1994).
[30] H. Zhang and H. Sato, Phys. Rev. Lett. **70**, 1697 (1993).
[31] A. Sokol, J. Phys. Chem. Solids **56**, 1673 (1995).
[32] J.L. Peng, P. Klavins, R.N. Shelton, H.B. Radousky, P.A. Hahn, and L. Bernardez, Phys. Rev. B **40**, 4517 (1989).
[33] C.L. Seaman, J.J. Neumeier, M.B. Maple, L.P. Le, G.M. Luke, B.J. Sternlieb, Y.J. Uemura, J.H. Brewer, R. Kadono, R.F. Kiefl, S.R. Krietzman, and T.M. Riseman, Phys. Rev. B **42**, 6801 (1990).
[34] J. Fink, N. Nücker, H. Romberg, M. Alexander, M.B. Maple, J.J. Neumeier, and J.W. Allen, Phys. Rev. B **42**, 4823 (1990).
[35] J.B. Torrance and R.M. Metzger, Phys. Rev. Lett. **63**, 1515 (1989).
[36] W. Jiang, J.L. Peng, S.H. Hagen, and R.L. Greene, Phys. Rev. B **46**, 8694 (1992).
[37] R. Fehrenbacher and T. Rice, Phys. Rev. Lett. **70**, 3471 (1993).
[38] A. Liechtenstein and I. Mazin, Phys. Rev. Lett. **74**, 1000 (1995).
[39] J. Clayhold, S. Hagen, Z.Z. Wang, N.P. Ong, J.M. Tarascon, and P. Barboux, Phys. Rev. B **39**, 777 (1989).
[40] T.R. Chien, Z.Z. Wang, and N.P. Ong, Phys. Rev. Lett. **67**, 2088 (1991).
[41] A. Matsuda, K. Kinoshita, T. Ishii, H. Shibita, T. Watanabe, and T. Yamada, Phys. Rev. B **38**, 2910 (1988).
[42] A. Carrington, D.J.C. Walker, A.P. Mackenzie, and J.R. Cooper, Phys. Rev. Lett. **69**, 2855 (1992)
[43] I. Felner, I. Nowik, E.R. Bauminger, D. Hechel, and U. Yaron, Phys. Rev. Lett. **65**, 1945 (1990).